

Novel Fast Lithium Ion Conduction in Garnet-Type $\text{Li}_5\text{La}_3\text{M}_2\text{O}_{12}$ ($\text{M} = \text{Nb}, \text{Ta}$)

Venkataraman Thangadurai, Heiko Kaack, and Werner J. F. Weppner*

Chair for Sensors and Solid State Ionics Faculty of Engineering, University of Kiel, Kaiserstrasse 2, 24143 Kiel, Germany

Lithium metal oxides with the nominal composition $\text{Li}_5\text{La}_3\text{M}_2\text{O}_{12}$ ($\text{M} = \text{Nb}, \text{Ta}$), possessing a garnetlike structure, have been investigated with regard to their electrical properties. These compounds form a new class of solid-state lithium ion conductors with a different crystal structure compared with all those known so far. The materials are prepared by solid-state reaction and characterized by powder XRD and ac impedance to determine their lithium ionic conductivity. Both the niobium and tantalum members exhibit the same order of magnitude of bulk conductivity ($\sim 10^{-6}$ S/cm at 25°C). The activation energies for ionic conductivity ($< 300^\circ\text{C}$) are 0.43 and 0.56 eV for $\text{Li}_5\text{La}_3\text{Nb}_2\text{O}_{12}$ and $\text{Li}_5\text{La}_3\text{Ta}_2\text{O}_{12}$, respectively, which are comparable to those of other solid lithium conductors, such as Lisicon, $\text{Li}_{14}\text{ZnGe}_4\text{O}_{16}$. Among the investigated materials, the tantalum compound $\text{Li}_5\text{La}_3\text{Ta}_2\text{O}_{12}$ is stable against reaction with molten lithium. Further tailoring of the compositions by appropriate chemical substitutions and improved synthesizing methods, especially with regard to minimizing grain-boundary resistance, are important issues in view of the potential use of the new class of compounds as electrolytes in practical lithium ion batteries.

I. Introduction

THERE is presently a strong ongoing search for materials for energy conversion^{1,2} and storage.^{3,4} e.g., both high- and low-temperature fuel cell electrolytes, photoelectrochemical solar cells, high-energy-density rechargeable (secondary) alkali-ion batteries, and hydrogen storage materials. Among these applications, rechargeable lithium batteries using lithium ion conducting electrolytes have drawn much attention due to their wide range use in portable electronic devices.⁴ The lithium ion battery is attractive because it has the highest energy density compared with other battery systems.⁵

To date, lithium ion secondary battery developments are mainly based on LiCoO_2 as the positive electrode, lithium ion conducting organic polymer as the electrolyte (LiPF_6 dissolved in polyethylene oxide), and lithium metal or graphite as the anode.^{5,6} The formation of a solid electrolyte interface⁷ at the anode leads to large irreversible capacity loss during the discharge cycles. A further major concern is the safety aspect of the liquid and common polymeric electrolytes.⁵ Thus, the development of alternative solid-state lithium ion conductors is an important issue for the present-day development of all-solid-state batteries.

So far, lithium ion conduction has been reported for a wide range of crystalline metal oxides and halides with different types of structure,^{8–12} such as $\text{Li}_{14}\text{ZnGe}_4\text{O}_{16}$ (Lisicon),^{13,14} Li_3N ,¹⁵

$\text{Li}-\beta$ -alumina,^{16,17} nasicon-type $\text{Li}_{1.3}\text{Ti}_{1.7}\text{Al}_{0.3}(\text{PO}_4)_3$,^{9,11} Li_2SiO_4 ,⁸ Li_3PO_4 , and perovskite-type $(\text{Li},\text{La})\text{TiO}_3$.^{18–21} Table I lists the most well-known crystalline lithium ion conductors and indicates their technical problems when being used as electrolytes in all-solid-state secondary battery applications.^{12–25} None of them is suitable for this purpose except $\text{Li}_{2.88}\text{PO}_{3.73}\text{N}_{0.14}$ (LiPON)²³ prepared *in situ* by a sputtering technique using a target of Li_3PO_4 in controlled N_2 atmosphere.²⁴

In our search for new solid-state lithium ion conductors possessing ideal chemical compositions with possible application in secondary batteries, we have investigated compounds with similar constituents, as in the case of the best lithium ion conductor $(\text{Li},\text{La})\text{TiO}_3$, but without lithium-reducible titanium and other metal ions, such as niobium, tungsten, molybdenum, or vanadium. Indeed, compounds with the general formula $\text{Li}_5\text{La}_3\text{M}_2\text{O}_{12}$ ($\text{M} = \text{Nb}, \text{Ta}$)^{26–28} are identified to have a garnetlike structure ($a = 12.889(3)$ Å for niobium and $12.823(2)$ for tantalum; space group $la\bar{3}d$). The structure is constructed of infinite chains of $(\text{La}_3\text{M}_2\text{O}_{12})_n$, which are oriented in four different directions, and the chains are bonded to each other by sharing lanthanum and lithium atoms.²⁷ These structural findings agree with the structure of two different chemical compositions, $\text{Li}_5\text{La}_3\text{M}_2\text{O}_{12}$ and $\text{Li}_7\text{La}_3\text{M}_2\text{O}_{13}$, reported in the literature.^{26–28} It is also suggested that lithium ion sites are not completely occupied in the first series while, in the latter, lithium sites are filled completely. Accordingly, it is expected that compounds with the formula $\text{Li}_5\text{La}_3\text{M}_2\text{O}_{12}$ may exhibit good lithium ionic conductivity. Indeed, the present study shows that garnet-type $\text{Li}_5\text{La}_3\text{M}_2\text{O}_{12}$ ($\text{M} = \text{Nb}, \text{Ta}$) forms a new family of fast lithium ion conductors with a different crystal structure compared with all known lithium ion conductors so far. The ionic conductivity is higher than those of LiPON, $\text{Li}_6\text{AlSiO}_8$, and $\text{Li}-\beta$ -alumina. Unlike $\text{Li}-\beta$ -alumina, the investigated garnet is a stoichiometric and isotropic compound and does not get hydrated. Optimization of the synthesis conditions as well as the composition appears to be promising for further improvement since tantalum is less reducible than other transition metals by lithium metal in view of practical applications in secondary lithium ion batteries.

II. Experimental Procedure

The title compounds were prepared by solid-state reaction using stoichiometric amounts of $\text{La}(\text{NO}_3)_3 \cdot 6\text{H}_2\text{O}$, $\text{LiOH} \cdot \text{H}_2\text{O}$, and M_2O_5 ($\text{M} = \text{Nb}, \text{Ta}$) at elevated temperature (Table II). After each stage of heat treatment, the powders were ball-milled using zirconia balls for ~ 12 h in 2-propanol. In the final stage of heat treatment, the reaction products were pressed into pellets by isostatic pressure. Powder XRD (XRD) (Model 3000, SEIFERT; $\text{CuK}\alpha$ radiation) was used at room temperature to monitor the phase formation after each sintering step. The lattice constant was obtained by least-squares refinement of the XRD data and was compared in Table II with the reported literature data.

Electrical conductivity measurements of the pellets (0.2 cm in thickness and 0.95 cm in diameter), sintered for 24 h at 950°C in air, were performed using lithium ion blocking gold electrodes (cured at 700°C for 1 h) in the temperature range from 25° to

B. Dunn—contributing editor

Manuscript No. 18696-4. Received May 16, 2002; approved October 21, 2002.

Work supported by research fellowship from the AvH-Foundation.

*Member, American Ceramic Society.

Table I. Typical Crystalline Lithium Ion Conductors Reported in the Literature and Their Properties

Electrolytes	Structure types	Reported year	Limiting factors in solid-state battery	Reference(s)
Li ₃ N	2-D (layered)	1977	Very low decomposition voltage (0.44 V)	15
Li-β-alumina	2-D (layered)	1967	Highly hygroscopic, difficult to prepare as pure phase	12, 16, 17
Li _{1.2} ZnGe ₂ O ₁₆ (Lisicon)	3-D	1978	Highly reactive with lithium metal, atmospheric CO ₂ ; conductivity decreases with time	13, 14
Li _{1.3} Ti _{1.7} Al _{0.3} (PO ₄) ₃	3-D	1989–90	Unstable with lithium metal, because of facile Ti ³⁺ reduction	9, 12, 22
(Li _{1.4})TiO ₃ (Perovskite-type)	3-D	1993	Unstable with lithium metal, because of facile Ti ³⁺ reduction, high temperature required for preparation, high loss of Li ₂ O, variance of conductivity with lithium concentration, difficulty in controlling lithium content	12, 18–21
Li _{2.88} PO _{3.86} N _{0.14} (LiPON)	3-D	1995	Moderate conductivity, used in development of thin-film battery, prepared using sputtering method <i>in situ</i>	23, 24
Li ₉ AlSiO ₈	3-D	1996	Moderate conductivity at room temperature, stable against lithium	25

600°C using an impedance and gain-phase analyzer (Model HP 4192 A, Hewlett-Packard Co., Palo Alto, CA) (5 Hz–13 MHz) interfaced with a PC (IBM Instruments, Inc., Danbury, CT). A two-probe cell was used for these measurements. Before each impedance measurement, the samples were equilibrated for 3–6 h at constant temperature. For each sample, the measurements were made for two heating and cooling cycles. The chemical stability of the investigated lithium ion conducting garnet-type oxides against reaction with molten lithium metal was tested in an argon-filled glove box.

III. Results and Discussion

Powder XRD patterns of the prepared metal oxides with the nominal composition Li₃La₃M₂O₁₂ (M = Nb, Ta) are similar to the reported values in the literature (Table II) and indicate the formation of garnet-type phases.^{26–28} Very interestingly, we found that the preparation of Li₇La₃Nb₂O₁₃ shows only the Li₃La₃Nb₂O₁₂ XRD pattern (Powder Diffraction File 84-1753, International Centre for Diffraction Data, Newtown Square, PA), which is different from the XRD pattern of Li₇La₃Nb₂O₁₃ (Powder Diffraction File 40-894). We could index the diffraction pattern on a cubic cell with a lattice constant of $a = 12.801(2)$ Å.

A typical impedance plot obtained for Li₃La₃Ta₂O₁₂ in air at 40°C is shown in Fig. 1. It is similar to that of the perovskite-type lithium ion conductor (Li_{1.4})TiO₃¹⁸ and β-alumina,²⁹ showing very small bulk (grain interior) resistance at the high-frequency side, and a slightly larger grain-boundary contribution and a tail at the low-frequency side, suggesting blocking of the electrodes for the mobile ions (lithium). The corresponding niobium member shows almost similar impedance data, except that both bulk and grain-boundary contributions are overlapping at the high-frequency side. The appearance of a low-frequency side tail is a first indication that the investigated garnet-type material is ionic in nature.

We could resolve the low-temperature (<110°C) impedance data into bulk, grain-boundary, and electrode effects using the program EQUIVALENT circuit³⁰ (Fig. 1 inset). The magnitude of

the capacitance of the bulk crystal and grain-boundary region is of the order of 1 pF and 7 nF, respectively. Because the contributions of the bulk and the grain boundary cannot be resolved over a wide range of temperature, we uniformly use all temperatures of the minimum negative imaginary value or intercept of the impedance plot with regard to the imaginary axis at the low-frequency side, which combines both bulk and grain-boundary contributions. Accordingly, the conductivity value reported here is the lower estimate of the true bulk conductivity of the materials.

Figure 2 shows a typical impedance plot for Li₃La₃Ta₂O₁₂ in air with reversible lithium electrodes (LiCoO₂). The appearance of the low-frequency intercept in this case is a second and more definite indication of lithium ion conduction in the investigated garnet-type materials. We also observe nearly the same bulk contributions to the total conductivity using reversible and nonreversible electrodes (Figs. 1 and 2). In the case of the reversible electrode, the grain-boundary portion is slightly overlapped by the electrode contribution.

Figure 3 shows the Arrhenius plot for the total (bulk + grain-boundary) ionic conductivity of Li₃La₃M₂O₁₂ (M = Nb, Ta). Both Li₃La₃Nb₂O₁₂ and Li₇La₃Nb₂O₁₃ exhibit a similar conductivity value. The conductivity data obtained from the heating and cooling cycle follow the same line, suggesting equilibrium conductivity behavior. The activation energies for electrical conductivity (<300°C) are 0.43 and 0.56 eV for Li₃La₃Nb₂O₁₂ and Li₃La₃Ta₂O₁₂, respectively, which are comparable to the values previously reported for the lithium ion conductor Lisicon (0.56 eV)¹⁴ and higher than the values for Li₃N (0.25 eV).¹⁵ The conductivity of Li₃La₃Ta₂O₁₂ is comparable to that of Li-β-alumina¹³ and Li₉AlSiO₈,²⁵ much higher than that of thick pellet LiPON,²³ and slightly lower than that of Li_{1.4}ZnGe₂O₁₆¹³ and Li_{0.34}La_{0.51}TiO_{2.94}³¹ (Fig. 4).

The dc conductivity value obtained from ac impedance data (Fig. 2) using the intercept close to the 5 Hz value, when employing reversible LiCoO₂ electrodes, shows that the dc conductivity of Li₃La₃Ta₂O₁₂ at 25°C is 1.2×10^{-6} S/cm, and total conductivity is 3.4×10^{-6} S/cm, which is a most attractive feature

Table II. Synthesis Conditions and Comparison of Lattice Parameters of Garnet-Type Li₃La₃M₂O₁₂ (M = Nb, Ta)

Compound	Synthesis conditions ¹	Lattice parameter (Å)
Li ₃ La ₃ Nb ₂ O ₁₂	700°C/24 h, 800°C/24 h, 850°C/12 h, and 950°C/24 h	12.762(3)
Li ₃ La ₃ Ta ₂ O ₁₂	700°C/24 h, 800°C/24 h, 850°C/12 h, and 950°C/24 h	12.766(3)
Li ₃ La ₃ Nb ₂ O ₁₂	500°C–850°C/6 h	12.797 ⁸
Li ₃ La ₃ Nb ₂ O ₁₂	700°C–900°C/24 h	12.889(3) ⁹
Li ₃ La ₃ Ta ₂ O ₁₂	500°C–850°C/6 h	12.804 ⁸
Li ₃ La ₃ Nb ₂ O ₁₂	700°C–900°C/24 h	12.823(2) ⁹

¹TG analysis of the synthesized compounds reveals that the compounds are stable up to 1000°C. ²Powder XRD patterns recorded after 800°C show the formation of a single-phase garnet structure. Further annealing was performed for sintering for electrical measurements. Above 1050°C, the samples were decomposed to perovskite-type La₃LiMO₆ (M = Nb, Ta) (ICDD Powder Diffraction File 40-895 and 39-897) and unidentified impurity. ³From Hyonma and Hayashi. ²⁷From Mazza. ²⁸

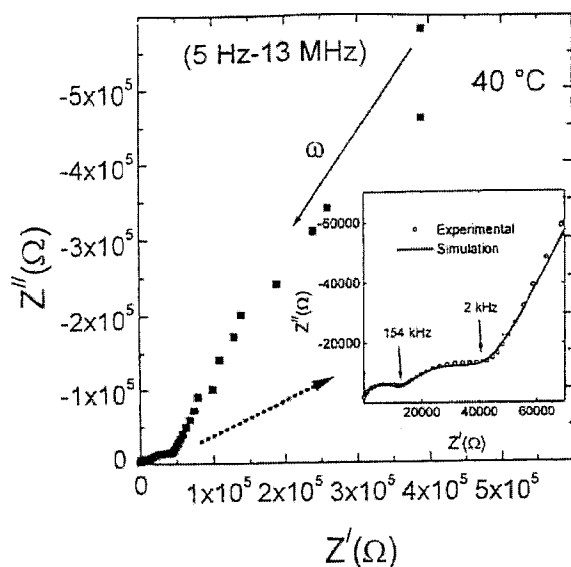


Fig. 1. Plot showing ac impedance data for $\text{Li}_5\text{La}_3\text{Ta}_2\text{O}_{12}$ using lithium ion blocking gold electrode. Applied voltage is 100 mV. Small bulk resistance is observed at high-frequency side. Grain-boundary contributions and tail are observed at low-frequency side. Inset shows expansion of high-frequency portion of the impedance spectrum. Line connecting data points has been fitted (using the EQUIVALENT program)³⁴ with an equivalent circuit consisting of two parallel resistance-capacitance and capacitance contributions $(RQ)(RQ)(Q)$.

of the investigated material compared with other lithium ion conductors. For comparison, the best lithium ion conductor based on perovskite ($\text{Li}(\text{La})\text{TiO}_3$) exhibits a total conductivity of $7 \times 10^{-5} \text{ S/cm}$ at 25°C , although its bulk conductivity is $\leq 1 \times 10^{-5} \text{ S/cm}$.¹⁸

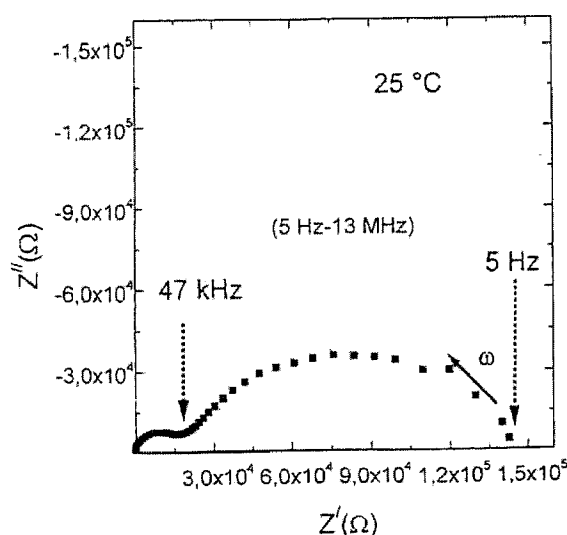


Fig. 2. Plot showing ac impedance data for $\text{Li}_5\text{La}_3\text{Ta}_2\text{O}_{12}$ using Li^+ ion reversible electrode (LiCoO_2). Applied signal voltage is 100 mV. Small bulk and grain-boundary contributions are observed at the high-frequency side, and a large intercept at the low-frequency side is observed due to the electrode, suggesting predominant lithium ion conduction. Bulk and total conductivity obtained from the high- and low-frequency intercept are of the same order of magnitude.

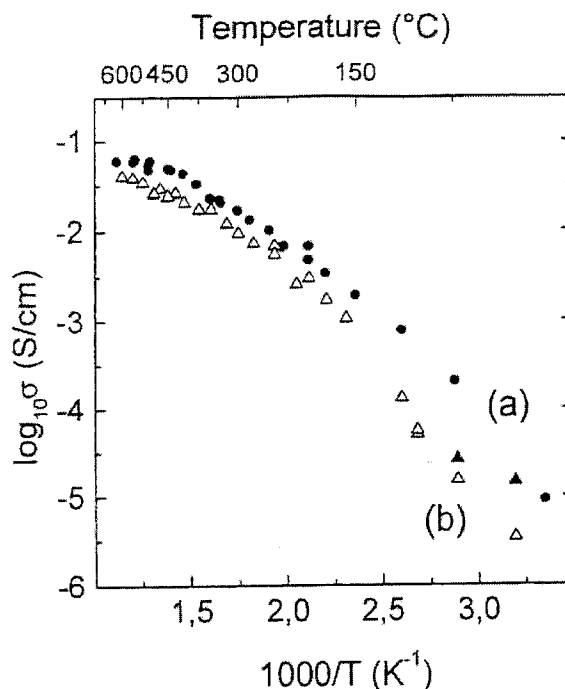


Fig. 3. Arrhenius plot for total (bulk + grain-boundary) conductivity of (a) $\text{Li}_5\text{La}_3\text{Nb}_2\text{O}_{12}$ (solid circles) and (b) $\text{Li}_5\text{La}_3\text{Ta}_2\text{O}_{12}$ (open triangles). Data obtained from the first heating and cooling cycle follow on the same line. Solid triangles represent the bulk ionic contribution of $\text{Li}_5\text{La}_3\text{Ta}_2\text{O}_{12}$. Both bulk and grain-boundary conductivity are nearly in the same order.

The high ionic conductivity in the present class of materials may be due to the migration of lithium ions in the three-dimensional framework. This is different from most of the well-known lithium ion conductors,⁸⁻¹² which have been observed mainly based on layered (two-dimensional) (Li_3N , Li- β -alumina), framework/nasicon-type ($\text{Li}_{1.3}\text{Ti}_{1.7}\text{Al}_{0.3}(\text{PO}_4)_3$ (open channel)), interstitial ($\text{Li}_{14}\text{ZnGe}_4\text{O}_{16}$), and defective perovskite ($(\text{Li},\text{La})\text{TiO}_3$) structures. In contrast to Li- β -alumina and Li_3N , the garnet is an isotropic (three-dimensional) compound, and hence conductivity occurs in three dimensions, similar to the case of nasicon-type and Lisicon lithium ion conductors. The exact mechanism for conduction is presently not known, however.

We investigated the chemical reaction stability of the tantalum compound $\text{Li}_5\text{La}_3\text{Ta}_2\text{O}_{12}$ with elemental lithium because it is composed of tantalum and lanthanum, which are less reducible^{34,35} than the niobium compound. Indeed, in contact with molten lithium, $\text{Li}_5\text{La}_3\text{Ta}_2\text{O}_{12}$ remains the original white color and does not show any signs of attack, suggesting that it is stable against reaction with elemental lithium. Accordingly, $\text{Li}_5\text{La}_3\text{Ta}_2\text{O}_{12}$ is considered to be a potential material for all-solid-state lithium ion batteries.

IV. Conclusions

The present studies show that the investigated garnet-type materials form an attractive new class of materials with fast lithium ion conduction comparable to other lithium ion conductors. More importantly, unlike fast lithium ion conducting $\text{Li}_{14}\text{ZnGe}_4\text{O}_{16}$, $(\text{Li},\text{La})\text{TiO}_3$, and $\text{Li}_{1.3}\text{Ti}_{1.7}\text{Al}_{0.3}(\text{PO}_4)_3$, one of the members of the garnets investigated here, $\text{Li}_5\text{La}_3\text{Ta}_2\text{O}_{12}$, is composed of tantalum and lanthanum, which are less reducible by lithium metal than other cationic species. Thus, further tailoring of the compositions by appropriate chemical substitutions and improved synthesizing methods, especially with regard to minimizing grain-boundary resistance, are important issues in view of using this electrolyte in practical lithium ion batteries.

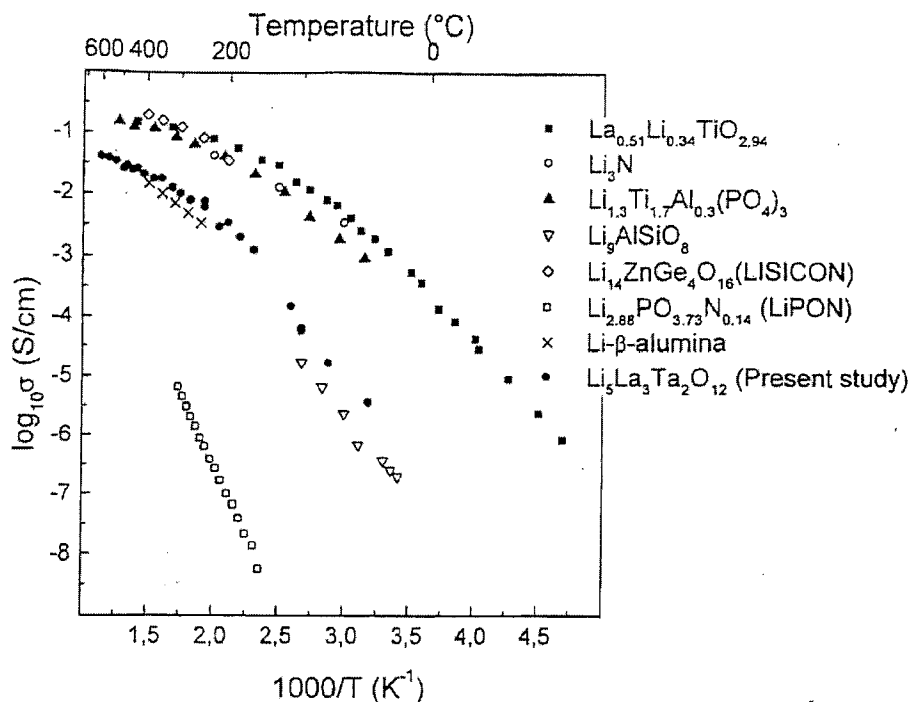


Fig. 4. Comparison of total conductivity of $\text{Li}_5\text{La}_3\text{Ta}_2\text{O}_{12}$ with other well-known lithium ion conductors reported in literature. Conductivity is higher than that of Li- β -alumina and LiPON, and it is comparable to that of perovskite-type ($\text{Li}_x\text{La}_{1-x}\text{TiO}_3$) and Lisicon.

References

1. B. C. H. Steele and A. Heinzel, "Materials for Fuel-Cell Technologies," *Nature (London)*, **414**, 345–52 (2001).
2. M. Gratzel, "Photoelectrochemical Cells," *Nature (London)*, **414**, 338–44 (2001).
3. L. Schlapbach and A. Züttel, "Hydrogen-Storage Materials for Mobile Applications," *Nature (London)*, **414**, 353–58 (2001).
4. J. M. Tarascon and M. Armand, "Issues and Challenges Facing Rechargeable Lithium Batteries," *Nature (London)*, **414**, 359–67 (2001).
5. J. R. Owen, "Rechargeable Lithium Batteries," *Chem. Soc. Rev.*, **26**, 259–67 (1997).
6. M. Wakihara and O. Yamamoto (Eds.), *Lithium Ion Batteries: Fundamentals and Performance*, Wiley-VCH, Weinheim, Germany, 1998.
7. M. Winter, J. O. Besenhard, M. E. Spahr, and P. Novak, "Insertion Electrode Materials for Rechargeable Lithium Batteries," *Adv. Mater.*, **10**, 725–63 (1998).
8. J. T. S. Irvine and A. R. West, "Crystalline Lithium Ion Conductors," pp. 201–23 in *High Conductivity Ionic Conductors, Recent Trends and Application*, Edited by T. Takahashi, World Scientific, Singapore, 1989.
9. H. Aono, H. Imanaka, and G. Y. Adachi, "High Li⁺ Conducting Ceramics," *Acc. Chem. Res.*, **27**, 265–70 (1994).
10. A. R. West, "Crystalline Solid Electrolytes I: General Considerations and the Major Materials," pp. 7–42 in *Solid-State Electrochemistry*, Edited by P. G. Bruce, Cambridge Press, Oxford, U.K., 1995.
11. G. Y. Adachi, H. Imanaka, and H. Aono, "Fast Li⁺ Conducting Ceramic Electrolytes," *Adv. Mater.*, **8**, 127–35 (1996).
12. A. D. Robertson, A. R. West, and A. G. Ritchie, "Review of Crystalline Lithium Ion Conductors Suitable for High-Temperature Battery Applications," *Solid State Ionics*, **104**, 1–11 (1997).
13. H. Y. P. Hong, "Crystal Structure and Ionic Conductivity of $\text{Li}_{1-x}\text{Zn}(\text{GeO}_4)_x$ and Other New Li⁺ Superionic Conductors," *Mater. Res. Bull.*, **13**, 117–24 (1978).
14. U. von Alpen, M. F. Bell, W. Wichelhaus, K. Y. Cheung, and G. J. Dudley, "Ionic Conductivity of $\text{Li}_{1-x}\text{Zn}(\text{GeO}_4)_x$ (Lisicon)," *Electrochim. Acta*, **23**, 1395–97 (1978).
15. U. von Alpen, A. Rabenau, and G. H. Tatlat, "Ionic Conductivity in Li_3N Single Crystals," *Appl. Phys. Lett.*, **30**, 621–23 (1977).
16. Y. F. Y. Yao and J. T. Kummer, "Ion Exchange Properties of and Rates of Ionic Diffusion in Beta-Alumina," *J. Inorg. Nucl. Chem.*, **29**, 2453–75 (1967).
17. G. C. Farrington, B. S. Dunn, and J. L. Briant, "Li⁺ and Divalent Ion Conductivity in Beta and Beta' Alumina," *Solid State Ionics*, **3–4**, 405–408 (1981).
18. Y. Inaguma, C. Liqian, M. Itoh, T. Nakamura, T. Uchida, H. Ikuta, and W. Wakihara, "High Ionic Conductivity in Lithium Lanthanum Titanate," *Solid State Commun.*, **86**, 689–93 (1993).
19. H. Kawai and J. Kuwano, "Lithium Ion Conductivity of A-Site Deficient Perovskite Solid Solution $\text{La}_{0.67-x}\text{Li}_x\text{TiO}_3$," *J. Electrochem. Soc.*, **141**, L78–L79 (1994).
20. O. Bohnke, C. Bohnke, and J. L. Fourquet, "Mechanism of Ionic Conduction and Electrochemical Intercalation of Lithium into the Perovskite Lanthanum Lithium Titanate," *Solid State Ionics*, **91**, 21–31 (1996).
21. P. Birke, S. Scharner, R. A. Huggins, and W. Weppner, "Electrolytic Stability Limit and Rapid Lithium Insertion in the Fast-Ion-Conducting $\text{Li}_{0.25}\text{La}_{0.75}\text{TiO}_3$ Perovskite-Type Compound," *J. Electrochem. Soc.*, **144**, L167–L169 (1997).
22. A. K. Padhi, K. S. Nanjundaswamy, C. Masquelier, and J. B. Goodenough, "Mapping of Transition Metal Redox Energies in Phosphates with Nasicon Structure by Lithium Intercalation," *J. Electrochem. Soc.*, **144**, 2581–86 (1997).
23. B. Wang, B. C. Chakoumakos, B. C. Sales, B. S. Kwak, and J. B. Bates, "Synthesis, Crystal Structure, and Ionic Conductivity of a Polycrystalline Lithium Phosphorous Oxynitride with the γ - Li_3PO_4 Structure," *J. Solid State Chem.*, **115**, 313–23 (1995).
24. B. Bates, N. J. Dudney, B. Neudecker, A. Ueda, and C. D. Evans, "Thin-Film Lithium and Lithium-Ion Batteries," *Solid State Ionics*, **135**, 33–45 (2000).
25. B. J. Neudecker and W. Weppner, " $\text{Li}_5\text{SiAlO}_8$: A Lithium Ion Electrolyte for Voltages above 5.4 V," *J. Electrochem. Soc.*, **143**, 2198–203 (1996).
26. F. Abbattista, M. Vallino, and D. Mazza, "Remarks on the Binary Systems $\text{Li}_2\text{O}-\text{Me}_2\text{O}$ (Me = Nb, Ta)," *Mater. Res. Bull.*, **22**, 1019–27 (1987).
27. H. Hyoona and K. Hayashi, "Crystal Structures of $\text{Li}_5\text{La}_3\text{M}_2\text{O}_{12}$ (M = Nb, Ta)," *Mater. Res. Bull.*, **23**, 1399–407 (1988).
28. D. Mazza, "Remarks on a Ternary Phase in the $\text{La}_2\text{O}_3-\text{Me}_2\text{O}-\text{Li}_2\text{O}$ System (Me = Nb, Ta)," *Mater. Lett.*, **7**, 205–207 (1988).
29. R. D. Armstrong, T. Dickinson, and P. M. Willis, "The ac Impedance of Powdered and Sintered Solid Ionic Conductors," *Electroanalytical Chem. Interfacial Electrochem.*, **53**, 389–405 (1974).
30. B. A. Boukamp, "Equivalent Circuit," Rept. No. CT88/265/128/CT89/214/128, Version 4.55, 1997, Faculty of Chemical Technology, University of Twente, Enschede, The Netherlands, May 1989.
31. M. Itoh, Y. Inaguma, W. H. Jung, L. Chen, and T. Nakamura, "High Lithium Ion Conductivity in the Perovskite-Type Compounds $\text{Ln}_0.4\text{Li}_{0.6}\text{TiO}_3$ (Ln = La, Pr, Nd, Sm)," *Solid State Ionics*, **70/71**, 203–207 (1994).
32. H. Watanabe and J. Kuwano, "Formation of Perovskite Solid Solutions and Lithium Ion Conductivity in the Compositions, $\text{Li}_2\text{Sr}_{1-2x}\text{M}^{III}_{0.5-x}\text{Ta}_{0.5-x}\text{O}_3$ (M = Cr, Fe, Co, Al, Ga, In, Y)," *J. Power Sources*, **68**, 421–26 (1997).
33. V. Thangadurai, A. K. Shukla, and J. Gopalakrishnan, " $\text{LiSr}_{1-x}\text{B}_{0.5-x}\text{B}'_{0.5-x}\text{O}_6$ (B = Ti, Zr; B' = Nb, Ta): New Lithium Ion Conductors Based on the Perovskite Structure," *Chem. Mater.*, **11**, 835–39 (1999).